

# Chain-reaction cascades in surfactant monolayer buckling

Ajaykumar Gopal,<sup>1</sup> Vladimir A. Belyi,<sup>2</sup> Haim Diamant,<sup>3</sup> Thomas A. Witten,<sup>2</sup> and Ka Yee C. Lee<sup>1</sup>

<sup>1</sup>Department of Chemistry and James Franck Institute, University of Chicago, Chicago, Illinois 60637

<sup>2</sup>Department of Physics and James Franck Institute, University of Chicago, Chicago, Illinois 60637

<sup>3</sup>School of Chemistry, Raymond and Beverly Sackler Faculty of Exact Sciences, Tel Aviv University, Tel Aviv 69978, Israel  
(Dated: September 6, 2004)

Certain surfactant monolayers at the water{air interface have been found to undergo, at a critical surface pressure, a dynamic instability involving multiple long folds of micron width. We exploit the sharp monolayer translations accompanying folding events to acquire, using a combination of fluorescence microscopy and digital image analysis, detailed statistics concerning the folding dynamics. The motions have a broad distribution of magnitudes and narrow, non-Gaussian distributions of angles and durations. The statistics are consistent with the occurrence of cooperative cascades of folds, implying an autocatalytic process uncommon in the context of mechanical instability.

PACS numbers: 68.18.Jk, 64.60.Qb, 82.60.Nh, 87.68.+z

Surfactant monolayers are found in many systems containing water{air or water{oil interfaces where surface tension, wetting, or liquid-liquid stability are to be controlled [1]. In recent years a remarkable variety of three-dimensional structures have been discovered upon lateral compression of surfactant monolayers, including straight folds [2, 3, 4], convoluted folds [4, 5], and attached vesicular objects of various shapes [3]. These instabilities have distinctive length scales ranging between 0.1 and 10  $\mu\text{m}$ . Thus the predominant stress relaxation is neither at the molecular level, which would lead to breakage or dissolution [6], nor at the macroscopic one, which would lead to long-wavelength buckling [7]. Moreover, the transitions occur under a net tensile stress, i.e., at surface pressures smaller than the bare surface tension of water (72  $\text{mN/m}$ ). Though the actual relaxation mechanism is unknown, a plausible driving force may be bilayer cohesion, i.e., the preference of the hydrophobic surfactant tails to join rather than remain in contact with air [5]. Domain boundaries in biphasic monolayers or grain boundaries in monophasic ones entail nanoscale topographies, which should cause localized buckling at low enough, positive tension [8], thus lowering the nucleation barrier for bilayer cohesion.

Out of the newly observed structures, the straight folds stand out as essentially different, corresponding to a more solid-like, nonequilibrium response of the monolayer [2, 3, 4, 8]. They are observed at lower temperature and higher compression rate, occur at higher critical pressures ( $\sim 70 \text{ mN/m}$ ), and are anisotropic, i.e., aligned on average perpendicular to the compression direction. A fold comprises a piece of monolayer of micron width and macroscopic length probably bound into a bilayer strip (Fig. 1). The main obstacle in studying fold formation is that it is a nucleated event initiated at an unpredictable spot and lasting a fraction of a second. Very rarely is such an event captured inside the field of view as in Fig. 1. Nevertheless, whenever a fold forms elsewhere, the viewed piece of monolayer translates sharply

and uniformly. Watching the monolayer jump as a result of such events, one is struck by the uniformity and unidirectionality of the motion, in contrast with the monolayer heterogeneity. The statistical analysis presented below corroborates this impression, revealing such features as anomalously narrow distributions of translation angle and duration.

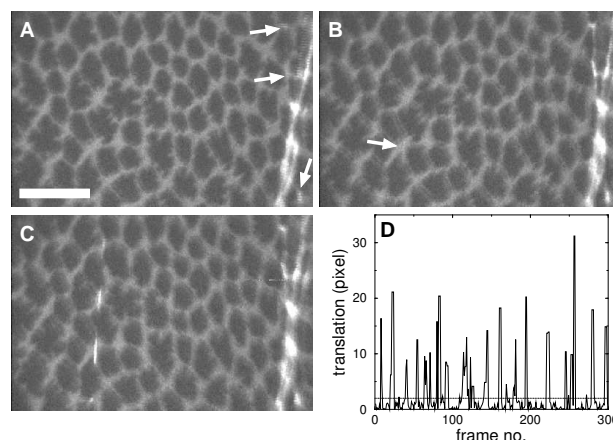


FIG. 1: (a)-(c) Fluorescence micrographs separated by 1/30 s intervals, showing the nearly-simultaneous formation of two folds. The images are blurred by monolayer motion. The scale bar length is 50  $\mu\text{m}$ . (d) Typical output of the tracking program, showing the monolayer translation within the field of view in sequential video frames. The spikes correspond to folding events occurring out of view. The dotted line shows the threshold used for event identification.

Insoluble monolayers containing a 7:3 mixture of dipalmitoylphosphocholine (DPPC) and palmitoylphosphoglycerol (POPG) were spread on the air{water interface from a chloroform solution at 25  $^{\circ}\text{C}$ . This was done on a rectangular Langmuir trough of maximum area 145  $\text{cm}^2$ , fitted with two mobile Teflon barriers of length 6.35 cm each, allowing for symmetric lateral compression. The phospholipids formed a low-density mono-

layer (area per molecule  $a > 100 \text{ \AA}^2$ ), exhibiting coexistence of two-dimensional gas and liquid phases. Lateral compression led, at a  $\dot{\gamma} \approx 67 \text{ s}^{-1}$ , to a homogeneous liquid phase followed, for a  $\dot{\gamma} < 65 \text{ s}^{-1}$ , by nucleation and growth of flower-like condensed domains (Fig. 1) until, at a  $\dot{\gamma} \approx 30 \text{ s}^{-1}$ , folding began. The relative barrier velocity was  $0.1 \text{ mm/s}$ , corresponding to compression rate of  $6.35 \text{ mm}^2/\text{s}$  and strain rate at the onset of folding of  $0.00154 \text{ s}^{-1}$ . Throughout the compression the morphology was observed using epifluorescence video microscopy and the surface tension monitored by a Wilhelmy surface balance. Further details of the apparatus can be found in Ref. [3]. The analog video was digitized into a series of 8-bit grayscale bitmaps of  $640 \times 480$  pixels at a rate of  $29.97 \text{ frames/s}$ . The series of images were then analyzed using a custom-made tracking program whose algorithm will be detailed elsewhere [9]. A typical output is shown in Fig. 1(d). Using a velocity threshold of 2 pixels per frame we identified 1817 events, recording for each its starting time, duration and total  $(l_x; l_y)$  translation.

Figure 2(a) shows the distribution of translations, exhibiting a broad tail: translations ten times the most probable one were observed. The distribution of on-times  $t$  (waiting times between events) is presented in Fig. 2(b). The mean on-time is  $\langle t \rangle = 0.31 \pm 0.01 \text{ s}$ , i.e., there are about three events per second. The histograms as well as an exponential distribution,  $p_t(t) = \langle t \rangle^{-1} e^{-t/\langle t \rangle}$ , consistent with a Poissonian, uncorrelated sequence of events. This conclusion is strengthened by a lack of correlation between  $l$  and the on-times before or after the event.

Figure 3(a) shows the distribution of translation angles  $\phi$ , where  $\tan \phi = l_y/l_x$ , and  $\phi = 0$  corresponds to motion parallel to the compression direction. The distribution is sharply peaked at  $\phi = 0$ , with standard deviation  $\sigma_{\phi} = 16.0 \pm 0.3^\circ$ . Folding is thus highly anisotropic, implying an elastic response of the monolayer within the folding time scale. This is in line with the viscoelasticity revealed by surface-rheology measurements in similar systems [5, 10], which yields relaxation times of order tens of seconds. One would expect a Gaussian distribution of fold angles because of either the combined effect of many scattering factors or a Boltzmann factor for the nucleation of a slanted fold with respect to the direction of maximum stress, whose energy increases as  $\sin^2 \phi$ . The peak of the measured distribution, however, is much sharper and clearly cannot be fitted by a Gaussian distribution (dotted curve). In Fig. 3(b) we show the mean angle  $\langle \phi \rangle$  of events as a function of their translation  $l$ . The two quantities are anticorrelated: larger events have smaller angles.

Figure 4(a) presents the distribution of on-times  $T$  (event durations). The distribution is narrow and asymmetric, yielding a mean on-time  $\langle T \rangle = 0.124 \pm 0.001 \text{ s}$  and standard deviation  $\sigma_T = 0.051 \pm 0.001 \text{ s}$ . The corresponding Gaussian distribution is depicted by the dotted line, highlighting the anomalous shape of the measured

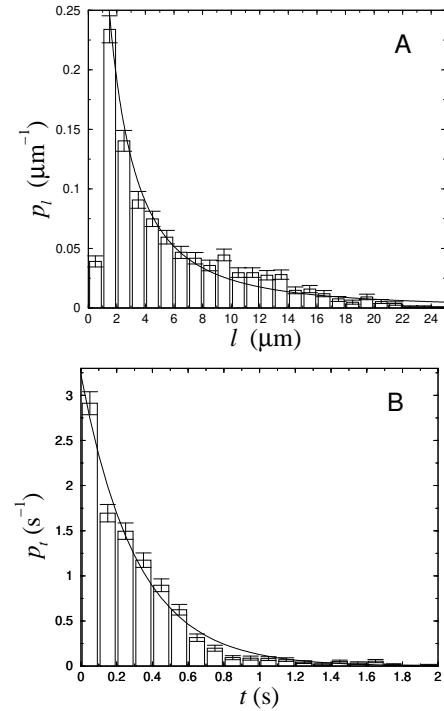


FIG. 2: (a) Distribution of translations. The solid line is obtained assuming a cascade mechanism [Eq. (2)]. (b) Distribution of on-times. The solid line shows an exponential distribution using the measured mean on-time  $\langle t \rangle = 0.31 \text{ s}$ .

distribution. The more moderate decrease to the right of the peak fits an exponential decay rather than a Gaussian one (inset). The narrow  $T$  distribution is surprising in view of the broad  $l$  distribution; one expects larger events to last longer. This correspondence is verified in Fig. 4(b), where the average on-time  $T_1$  is plotted as a function of the translation  $l$ . Yet, the increase of  $T_1$  with  $l$  is only logarithmic and, therefore, even very large translations do not have correspondingly long duration.

The broad distribution of translations can arise from two alternative scenarios: each observed event could correspond to either a single fold, whereby the folds have a broad distribution of sizes, or a cascade of roughly identical folds, the cascades having a broad distribution of magnitudes. The following analysis, as well as the handful of folds captured in the field of view, strongly support the latter scenario.

Let us assume that an observed event is caused by a cascade of  $n$  folds, each contributing roughly the same translation  $l_i$  and having an angle  $\phi_i$ ,  $i = 1 :: n$ . We assume for simplicity that the angles are drawn from independent Gaussian distributions having a standard deviation  $\sigma_{\phi_i}$ ,  $p_{\phi_i}(\phi_i) = (2\pi\sigma_{\phi_i}^2)^{-1/2} e^{-\phi_i^2/(2\sigma_{\phi_i}^2)}$ . The measured translation is the sum of contributions from all folds,  $l = \sum_{i=1}^n l_i$ , but the observed translation angle is the average of the individual fold angles,  $\phi = \frac{1}{n} \sum_{i=1}^n \phi_i$ . The distribution of  $\phi$  is therefore narrower the larger the

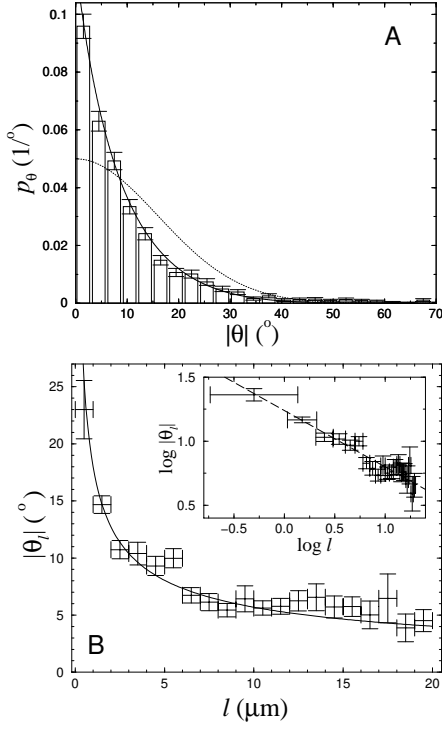


FIG. 3: (a) Distribution of translation angles. The dotted line shows a Gaussian distribution with the measured  $\sigma^2$ . The solid line is obtained assuming a cascade mechanism [Eq. (3)] with  $\alpha = 16$ . (b) Average angle of events whose translations fall within the same narrow range. The solid line is a fit to  $j_{1j} = l^{-1/2}$  [Eq. (1)] with  $\alpha = 18 \pm 3$  ( $\sigma = 1^{-1/2}$ ). The inset presents the same data on a  $\log\{\log$  scale, the dashed line being an error-weighted linear fit with a slope of  $0.44 \pm 0.05$ .

value of  $n$ ,  $p_n(n; \alpha) = [n(2^{-\alpha})]^{1/2} e^{-n(2^{-\alpha})}$ . This implies that, regardless of the distribution of  $l$ , the average absolute angle of events having the same translation  $l$  should decrease as  $l^{-1/2}$ ,

$$j_{1j} = [2^{-\alpha} l]^{1/2}; \quad (1)$$

which is consistent with the findings of Fig. 3(b). From the fit we get  $2^{-\alpha} l = 500 \pm 200$  ( $^\circ$ )<sup>2</sup> m. Thus, large cascades give rise to "focusing" onto small-angle translations. This effect, along with the broad  $l$  distribution, explains the large statistical weight of small angles.

Suppose that each fold takes a time  $T_1$  to complete and another time  $\tau$  to "topple" another fold. Consider a cascade made of  $g$  generations of topples, where each fold can topple  $q$  others [1]. The total on-time is  $T = T_1 + (g-1)\tau$ , and the total number of folds is  $n = g$  if  $q = 1$ , or  $n = (q^g - 1)/(q - 1)$  if  $q > 1$ . From these two equations and  $n' = l^{-1/2}$  we obtain a relation between the on-time  $T$  and the translation  $l$ ,  $T = (\tau/l^{1/2}) + T_1$  if  $q = 1$ , and  $T = (\tau/\ln q) \ln[(q-1)l^{-1/2} + 1] + T_1$  if  $q > 1$ . Thus, for low cooperativity ( $q = 1$ ) we expect  $T$  to depend linearly on  $l$ , whereas for larger cooperativity the dependence becomes logarithmic. As seen in Fig. 4(b),

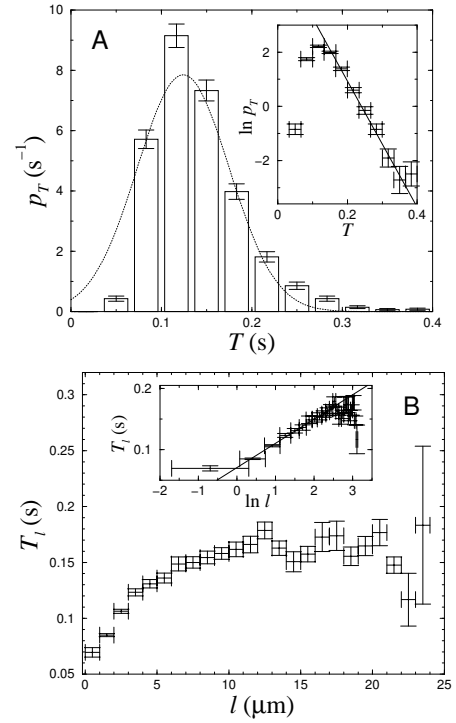


FIG. 4: (a) Distribution of on-times. The dotted line shows a Gaussian distribution using the measured mean and standard deviation. The inset presents the data on a  $\ln\{\ln$  scale, the solid line being an error-weighted linear fit with a slope of  $23.3 \pm 3$  s<sup>-1</sup>. (b) Average on-time of events whose translations fall within the same narrow range. The inset presents the same data on a  $\ln\{\ln$  scale, the solid line being an error-weighted linear fit with a slope of  $0.040 \pm 0.004$  s.

the results are consistent with the latter, i.e., the cascades are cooperative, one fold toppling several others.

Assuming a fixed probability to topple a generation of folds, we get an exponential distribution of  $g$ ,  $p_g(g) = [(1 - \alpha)]^g$ , and hence an exponential distribution of  $T$  for  $T > T_1$ . The statistics for  $T < T_1$  are determined by the scatter of  $T_1$ , which has been neglected so far. Hence,  $p_T(T)$  should have an asymmetric shape, dropping sharply for  $T < T_1$  and decaying exponentially for  $T > T_1$ . These conclusions agree with the measurements of Fig. 4(a), whereupon the distribution peak can be identified as the single-fold time,  $T_1 = 0.12 \pm 0.03$  s. From the first two moments of  $p_T(T > T_1)$  we extract  $\tau = 0.026 \pm 0.005$  s and  $\alpha = 0.54 \pm 0.05$ . Hence,  $\ln q = 1/(1 - \alpha) = 2.2 \pm 0.2$ , i.e., the cascades consist of 2.3 generations on average. From the linear fit in Fig. 4(b), whose slope is equal to  $\tau/\ln q$ , we get  $q = 1.9 \pm 0.2$ , i.e., each fold topples about two others. The cooperativity and short toppling time account for the uniformity of event duration: even the largest cascades involve only a few generations and do not last long.

Using the exponential distribution of  $g$  and the relation

between  $g$  and  $n$ , we find

$$p_n(n) = [(q-1)n+1]^{-1}; \quad \ln = \ln q; \quad (2)$$

The distribution of magnitudes tends for large  $n = l-1$  to a power law, the decay exponent being always smaller than 1. (For our system we get  $\ln = 2.0 \pm 0.2$ .) Using the expressions for  $p_n(n)$  and  $p_{n-1}(n)$  we can calculate the distribution of angles as  $p(j) = \sum_{n=1}^j p_n(n)p_{n-1}(n)$ , yielding

$$p(j) = N \sum_{n=1}^j [(q-1)n+1]^{-1} n^{1-2} e^{-n-2} (2^{-2})^{n-1}; \quad (3)$$

where  $N = 2(2^{-2})^{1-2} (q-1) = [q/(q-1)]$  is a normalization factor. This distribution reproduces well the focusing of the angular distribution, as shown by the solid line in Fig. 3(a). We note that, if one has in a certain system  $1 < \ln = \ln q < 2$  (i.e.,  $\ln = \ln q > 1=2$ ), Eq. (3) predicts an (integrable) singularity of  $p$  at  $j=0$ . The fit in Fig. 3(a) gives  $\ln = 1.6 \pm 0.2$  which, together with the estimate for  $l_1$  obtained from Fig. 3(b), yields  $l_1 = 2.0 \pm 0.8$  m. Finally, we use the values derived for  $l_1$ ,  $q$  and  $\ln$  to reproduce the translation distribution  $p_1$  according to Eq. (2). As shown by the solid line in Fig. 2(a), the calculated distribution gives a reasonable fit to the decaying part of  $p_1(l)$ . (The sharply increasing part is probably determined by the scatter of  $q$ .)

The cascade analysis provides a consistent account of the measured statistics. The alternative single-fold scenario, corresponding to  $n = g = 1$ , does not agree with the measurements and cannot account for the sharp distributions of angle and duration. The evidence for cooperative cascades, however, remains indirect. Our analysis implies that the folding transition follows unusual nucleation kinetics, in which single-fold growth is macroscopic in one dimension (length) but restricted in another (width). Consequently, a single nucleus cannot fully relax its super-stressed environment, thereby driving the nucleation of other folds in a chain-reaction manner. Such a process, resembling an autocatalytic chemical reaction or nuclear fission, has never been recognized, to the best of our knowledge, in the context of mechanical instability such as the buckling discussed here. Moreover, this scenario should not be restricted to our specific system but is to be expected whenever there is an autocatalytic instability whose evolution is limited for some reason to discrete units of relaxation.

A key question is what sets the scale of the restricted fold growth. Folding may introduce extra strain in the monolayer, e.g., as a result of mismatches in the rapidly folded region. This strain will increase with fold width, eventually balancing the cohesion energy and halting the folding. Another open issue is the mechanism of correlation between folds in a cascade. Toppling may be caused by the long-range stress field emanating from the tips of a propagating fold. This extra stress appears immediately after fold nucleation and can account for the short

toppling time inferred above. A complicated question to be addressed in a future publication [9] relates to the role of compression rate. It will be interesting to check what happens to the folding cascades when the compression is not unidirectional, e.g., in a circular trough [12].

This work was partially supported by the University of Chicago MRSEC program of the NSF (DMR-0213745) and the US-Israel Binational Science Foundation (2002-271). The experimental apparatus was made possible by an NSF CAREER/Junior Faculty Grant (CHE-9816513). K.Y.C.L. is grateful for the support from the March of Dimes (#6-FY03-58) and the Packard Foundation (99-1465). H.D. acknowledges support from the Israeli Council of Higher Education (Alon Fellowship).

---

Electronic address: hdiament@tau.ac.il

- [1] K.S.Birdi, Self-Assembly of Monolayer Structures of Lipids and Macromolecules at Interfaces, Plenum Press, New York, 1999.
- [2] M.M.Lipp, K.Y.C.Lee, J.A.Zasadzinski, and A.J.Waring, Science 273, 1196 (1996). M.M.Lipp, K.Y.C.Lee, A.J.Waring, and J.A.Zasadzinski, Biophys.J. 72, 2783 (1997). M.M.Lipp, K.Y.C.Lee, D.Y.Takamoto, J.A.Zasadzinski, and A.J.Waring, Phys.Rev.Lett. 81, 1650 (1998).
- [3] A.Gopal and K.Y.C.Lee, J.Phys.Chem.B 105, 10348 (2001).
- [4] C.Ybert, W.Lu, G.Moller, and C.M.Knobler, J.Phys.Chem.B 106, 2004 (2002); J.Phys.Cond.Mat. 14, 4753 (2002).
- [5] W.Lu, C.M.Knobler, R.F.Bruinsma, M.Twardos, and M.Dennin, Phys.Rev.Lett. 89, 146107 (2002).
- [6] L.Pauchard and J.Munier, Phys.Rev.Lett. 70, 3565 (1993); Phil.Mag.B 78, 221 (1998). E.Hatta, H.Hosoi, H.Akiyama, T.Ishii, and K.Mukasa, Eur.Phys.J.B 2, 347 (1998).
- [7] S.T.Miher, J.F.Joanny, and P.Pincus, Europhys.Lett. 9, 495 (1989).
- [8] H.Diamant, T.A.Witten, A.Gopal, and K.Y.C.Lee, Europhys.Lett. 52, 171 (2000). H.Diamant, T.A.Witten, C.Ege, A.Gopal, and K.Y.C.Lee, Phys.Rev.E 63, 061602 (2001).
- [9] A.Gopal, V.A.Belyi, H.Diamant, T.A.Witten, and K.Y.C.Lee, unpublished.
- [10] G.Kretzschmar, J.Li, R.Miller, H.Motschmann, and H.Mohwald, Colloid Surf.A 114, 277 (1996). J.Kragel, G.Kretzschmar, J.B.Lee, G.Loglio, R.Miller, and H.Mohwald, Thin Solid Films 284(285), 361 (1996). J.B.Lee, G.Kretzschmar, R.Miller, and H.Mohwald, Colloid Surf.A 149, 491 (1999).
- [11] Strictly speaking,  $T_1$  and  $q$  are stochastic variables. We assume that their distributions are much narrower than that of the cascade sizes.
- [12] R.S.Ghaskadvi and M.Dennin, Rev.Sci.Instrum. 69, 3568 (1998).